AD-A138 546 FACTORS INFLUENCING THERMOMECHANICAL FAILURE OF FACE SEALS III(U) THAYER SCHOOL OF ENGINEERING HANOVER N H F E KENNEDY ET AL. JAN 84 N00014-81-K-0090 1/1

UNCLASSIFIED F/G 11/1 NL

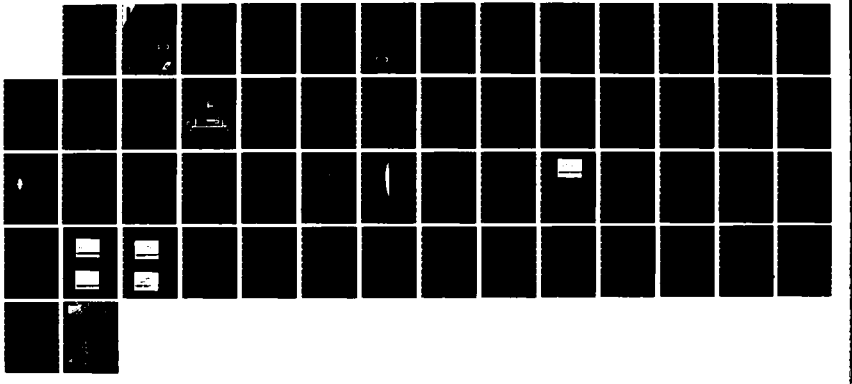

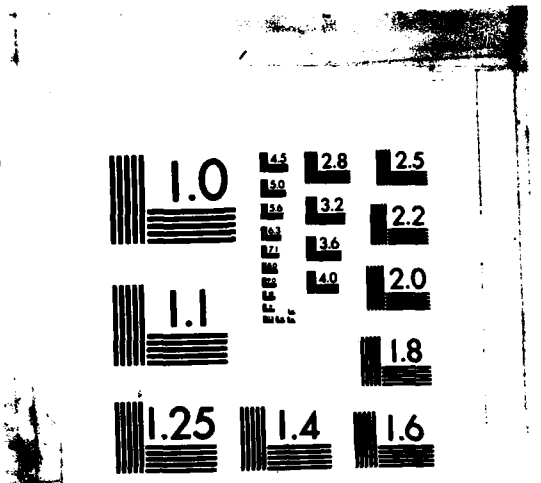

MICROCOPY RESOLUTION TEST CHART
NATIONAL BUREAU OF STANDARDS-1963-A

12

FACTORS INFLUENCING THERMOMECHANICAL FAILURE OF FACE SEALS III

by

F.E. Kennedy, Jr., C-K. Chuah, and W. Brote

ANNUAL REPORT

Office of Naval Research
Contract No. N00014-81-K-0090
Period Covered: December 1, 1982 - November 30, 1983

JANUARY 1984

THAYER SCHOOL OF ENGINEERING
a professional school of Dartmouth College
Hanover, New Hampshire 03755

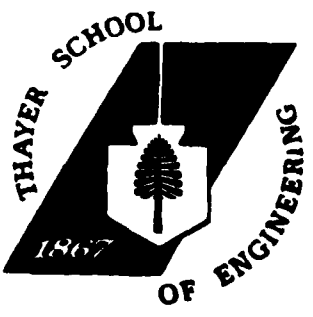

Unclassified

SECURITY CLASSIFICATION OF THIS PAGE (When Data Entered)

REPORT DOCUMENTATION PAGE		READ INSTRUCTIONS BEFORE COMPLETING FORM
1. REPORT NUMBER	2. GOVT ACCESSION NO. AD-A138546	3. RECIPIENT'S CATALOG NUMBER
4. TITLE (and Subtitle) FACTORS INFLUENCING THERMOMECHANICAL FAILURE OF FACE SEALS III		5. TYPE OF REPORT & PERIOD COVERED Annual Report Dec. 1, 1982-Nov. 30, 1983
		6. PERFORMING ORG. REPORT NUMBER
7. AUTHOR(s) Francis E. Kennedy, Jr. Chong-Khai Chuah Wilhelm Brote		8. CONTRACT OR GRANT NUMBER(s) N00014-81-K-0090
9. PERFORMING ORGANIZATION NAME AND ADDRESS Thayer School of Engineering Dartmouth College Hanover, New Hampshire 03755		10. PROGRAM ELEMENT, PROJECT, TASK AREA & WORK UNIT NUMBERS
11. CONTROLLING OFFICE NAME AND ADDRESS Engineering Science Directorate Office of Naval Research Arlington, Virginia 22217		12. REPORT DATE January 1984
		13. NUMBER OF PAGES
14. MONITORING AGENCY NAME & ADDRESS(if different from Controlling Office)		15. SECURITY CLASS. (of this report) Unclassified
		15a. DECLASSIFICATION/DOWNGRADING SCHEDULE

16. DISTRIBUTION STATEMENT (of this Report)

Approved for public release; distribution unlimited.

17. DISTRIBUTION STATEMENT (of the abstract entered in Block 20, if different from Report)

18. SUPPLEMENTARY NOTES

19. KEY WORDS (Continue on reverse side if necessary and identify by block number)

Mechanical Seals, Face Seals, Seals, Thermoelastic Instability, Failure, Surface Temperature, Wear.

20. ABSTRACT (Continue on reverse side if necessary and identify by block number)

Analytical and experimental studies of factors affecting thermocracking and other modes of thermomechanical failure of mechanical face seals have continued for a third year.

Mechanical face seals are assumed to operate with a uniform, thin film of sealed fluid between the flat, parallel seal faces. Recent evidence has indicated, however, that in many seals there exist patches of solid-to-solid contact between the seal faces. The temperatures and stresses near these concentrated contacts may be responsible for some modes of seal failure.

DD FORM 1 JAN 73 1473 EDITION OF 1 NOV 65 IS OBSOLETE S/N 0102-LF-014-6601

Unclassified

SECURITY CLASSIFICATION OF THIS PAGE (When Data Entered)

20 (continued)

In this study an experimental determination was made of the number, size, and location of contact patches in actual face seals operating with and without a sealed liquid. This information was used in a numerical analysis, using finite element techniques, of temperatures, deformations, and stresses around the contact patches. An independent experimental measurement of surface temperature profile within the contact patches was used to refine the numerical analysis and to enable determination of frictional heat flux and contact pressure distributions.

Measurements of seal ring surface profiles were compared with contact probe output to ascertain that the contact patches were located at waviness peaks on the metallic ring surface. Measurements of wear (mass loss) of the seal rings showed that carbon ring wear is much greater than that of the metallic ring surface and that both wear magnitudes are significantly affected by the wear resistance of the carbon ring material. Wear of the metallic face appears to be concentrated near the waviness peaks where contact patches are found. The contact conditions within those patches have an important influence on such potential seal failure mechanisms as wear, excessive plastic deformation, and thermocracking.

FACTORS INFLUENCING THERMOMECHANICAL FAILURE OF FACE SEALS III

Annual Report #3

submitted to

Office of Naval Research
Contract No. N00014-81-K-0090
Period Covered: December 1, 1982 to November 30, 1983

by

Francis E. Kennedy, Jr.
Associate Professor of Engineering

and

Chong-Khai Chuah and Wilhelm Brote
Graduate Research Assistants

Thayer School of Engineering
Dartmouth College
Hanover, New Hampshire 03755

January 1984

FOREWORD

Work at the Thayer School of Engineering at Dartmouth College on this project has been supported by Office of Naval Research Contract No. N00014-81-K-0090. Dr. A. William Ruff has been the ONR contract monitor since January 1, 1983, while Mr. M. Keith Ellingsworth of ONR was the contract monitor until December 31, 1982.

Mr. Victor A. Surprenant of Dartmouth College assisted in materials aspects of the research and both he and Sidney A. Karpe of the David Taylor Naval Ship R&D Center in Annapolis contributed measurably to discussions about the observed seal contact phenomena. Drs. Daniel F. Play of INSA, Lyon, France and Irving H. Thomae of Dartmouth College assisted in the development of the computer-based surface profilometry system.

Face seals for the experimental phase of the project were contributed by EG&G Sealol, Inc., H.F. Greiner, Vice President and Chief Engineer. Carbon composite seal rings for wear testing were provided by United Technologies Corp. Research Center, Dr. Eric J. Minford, Associate Research Scientist. Assistance with seal ring profile measurement was provided by personnel of Alphamicron, Inc., Lebanon, N.H.

TABLE OF CONTENTS

LIST OF FIGURES

LIST OF TABLES

INTRODUCTION AND BACKGROUND

Since December 1, 1980, work has been in progress at Thayer School of Engineering on ONR Contract N00014-81-K-0090. The goal of the work has been to gain a better understanding of factors affecting thermomechanical failure of seal rings in mechanical face seals. The research has been directed at learning the root causes of thermocracking and other failure modes, the relationship between the failure mechanisms and non-uniformity of contact at the seal interface, and what material parameters have the most influence on the failure mechanisms. The research has included both analytical and experimental activities aimed at accomplishing these goals. The results obtained in the first two years of this research program were described in earlier reports [1,2], but will be summarized here for completeness. This report will concentrate on work performed during the period December 1, 1982 to November 30, 1983.

The sealing interface of a mechanical face seal consists of two seal rings with their contacting surfaces lapped flat and parallel. It has been assumed that during operation the two seal faces, one of which is rotating and one stationary, either are in uniform, lightly loaded contact or else have a thin, uniform film of sealed fluid separating them. In actual fact, however, the seal surfaces have a slight initial waviness and this results in non-uniform solid-to-solid contact at the seal interface. One consequence of this is that frictional tractions and the resulting frictional heating can vary around the seal ring circumference. It was shown by Burton and others [3,5] that this non-uniform heating may, by the process known as thermoelastic instability, result in concentration of contact into a few hot, highly stressed contact patches or thermal asperities. At the outset of this work it was hypothesized that this concentration of contact could result in seal failure by thermocracking and other thermomechanical failure modes.

The first phase of the work, accomplished with the aid of personnel at

the David Taylor Naval Ship R & D Center in Annapolis, involved the examination of marine seal components which have exhibited thermocracking. Macroscopic and microscopic examination of the metallic seal rings showed that most thermocracks are radial in nature and initiate at carbide particles on the seal surface of the cast cobalt-based alloy rings [1,6]. The cracks, which are distributed relatively uniformly in the circumferential direction on the seal face, appear to initiate and propagate in a brittle manner in a tensile mode (Mode I). There was evidence on the seal surfaces that localized contact conditions had occurred in thermocracked regions, with both deformation and temperature in the contact region being rather severe.

The next phase of this research was an analytical study which aimed to determine how localized contact patches at the seal interface could lead to the onset of thermocracking. The finite element method was chosen and a finite element thermal analysis program was developed for use in calculating surface temperature distributions in sliding seals [7,8]. This program, THERMAP, was used along with a finite element stress analysis program, FEATS, to determine temperature and thermal stress distributions near contact patches on the seal ring surface [1,6]. It was found that very high temperatures occur at the contact patches owing to frictional heating. The regions affected by these high temperatures are quite small, but thermal stresses in those regions are large. The stresses are compressive, however, so cannot directly cause thermocracks of the type observed in our studies. It was concluded that these large compressive thermal stresses cause substantial plastic deformation near contact patches. Upon movement of the contact patch, residual tensile stress would result which could easily cause cracks like those observed [6].

The analytical study resulted in a proposed thermocrack mechanism which could account for the observed characteristics of thermocracks. The analysis relied, however, on a crucial assumption--that the formation of localized

contact patches, or thermoelastic instabilities, precedes thermocracking. Similar small, highly loaded contact patches had been observed in various laboratory configurations by other researchers [5,9], but there had been no direct observation of thermoelastic instabilities in face seals. There was some evidence, based on observation of disassembled seal faces after seal failure, that this was in fact what had occurred [10]. Not until recently, however, has the presence of the hot contact patches actually been detected in operating face seals. Recent work in our laboratory has resulted in the development of a contact probe which can be used in monitoring contact patch sizes and locations in ring-on-ring or ring-on-disk configurations [11]. The probe also serves as a dynamic thermocouple to enable measurement of surface temperatures within the contact patches. It has already proven quite effective in the characterization of contact patches in operating mechanical face seals, especially during dry operation [11,12].

Substantial evidence has been obtained which shows that contact in face seals, at least during dry operation, is concentrated in several small patches on the seal interface. In all cases the patches remain approximately stationary with respect to the metallic seal ring, whether that ring be stationary or rotating. The number of these patches is usually between 2 to 4 and their size is dependent on the properties of the seal materials and on the operating parameters, especially velocity of the seal. A dynamic thermocouple was developed to measure the temperatures within the contact patches and those temperatures, which were well above ambient temperature, were found to depend on the size of the contact patches as well as the amount of frictional heat generated within them [11,12]. The experimental work has, therefore, produced the first recorded data on contact conditions in operating face seals. Application of the contact probe to liquid lubricated face seals had however proven difficult and inconclusive [12]. One of the objectives of this past year's work was the extension

of the experimental study of seal contact conditions to liquid lubricated seals.

Several analysis of the stress and temperature distributions around contact patches in seal-like configuration have been attempted [6,13,14]. They have shown that both stress and surface temperature reach high values in the patch vicinity and that the stresses can be high enough to cause plastic deformation and cracking of the contacting seal faces in severe cases [6,14]. These analyses have, however, relied on assumptions about contact patch size and about the distribution of frictional heat flux and surface tractions. There had been no previous attempt to evaluate the contact conditions actually present in face seals and to determine the stress and temperature distributions under those conditions. Such a determination was a second objective of this past year's work on this project.

As was stated above, it was hypothesized that the origin of the non-uniform solid/solid contact conditions on the sealing surface is the initial waviness of the seal faces. This initial waviness has been found to be present despite careful lapping of the sealing surfaces [15]. Another objective of this year's work was the determination of the relationship between contact patch locations and the surface profile of the seal rings.

A final objective of this year's research was to begin a study of wear of the contacting seal ring surfaces. Earlier work on this project had not included any measurement of seal ring wear.

APPARATUS AND PROCEDURES

Experimental Apparatus for Contact Study

The seals used in this program were slightly modified versions of a mechanical face seal designed for turbine engine applications. The seal has a commercially-available carbon graphite primary ring, which in most of these tests served as the stationary seal ring. The rotating ring was metallic, with three different metal ring materials being used in the study: 440 C stainless steel, beryllium copper, and 52100 bearing steel. The properties of the metallic ring materials are given in Table 1. The sealing surface had an inside diameter of 5 cm and a width of 2.5 mm.

The seal rings were mounted in specially designed holders. The holder with the rotating ring was mounted on the spindle of a modified drill press. The stationary specimen holder was mounted on a thrust bearing beneath the spindle and was surrounded by a test chamber which could serve to collect leakage from the seal. Rotation of the test chamber was limited by a torque-sensing system for friction determination. Normal load was applied through the spindle by a static weight hung on the loading arm. The spindle was rotated at a preset speed ranging from 15.7 rad/s to 188.5 rad/s (surface velocity of the rotating ring ranging from 0.41 to 4.95 m/s).

The stationary carbon seal ring had a very small (0.22 mm diameter) hole drilled in it, perpendicular to the contact surface. A fine wire (.18 mm diameter) was mounted in the hole to act as a contact probe [11]. The wire was bonded in the ring with an electrically insulating adhesive and the surface of the ring was then lapped and polished. The wire then formed part of the seal ring surface, but it was electrically insulated from the rest of the ring. The probe wire was made from constantan so that it could act as one leg of a dynamic thermocouple [11]. The other side of the contact probe circuit, and the other leg of the thermocouple,

was the rotating metallic seal ring. Electrical connection was made to the rotating seal ring through a carbon electrical brush at the ring outside diameter. A schematic diagram of the test apparatus is shown in Figure 1.

To allow the possibility of liquid lubricated seal tests, a means was provided to supply pressurized fluid to the interior of the seal. For the purposes of these tests, the fluid was tap-water and its pressure could be controlled by a regulator in the supply line (Figure 1). The flexible supply line tubing did not inhibit friction measurement.

During a test, the contact probe/thermocouple worked as follows [11]: In the probe mode, a 5 volt D.C. signal was applied to the rotating ring via the electrical brush. The probe wire was monitored using an oscilloscope. If the wire location on the stationary ring was in intimate contact with the rotating ring, a 5 volt signal appeared on the scope; otherwise zero volts appeared. The oscilloscope trace was triggered at the same point on the rotating ring each revolution. The probe output could, therefore, be used to locate contact patches, determine their size (from the width of the 5 V pulses) and monitor their motion relative to the moving ring. In the thermocouple mode the 5 V input signal was turned off and, instead, the emf generated by the dynamic thermocouple junction was monitored, enabling temperatures of the contact patches to be approximated. In order to completely map the contact patch motion, the ring positions were switched; a probe wire was mounted in the previously-rotating ring, and the test was repeated.

Wear measurements were made during some of the dry tests. These were done by weighing both seal rings before and after the tests, which were run for a set duration (1 hour). Wear was therefore measured as weight (or mass) loss during a test run. No attempt was made to pinpoint the location of wear activity on the surfaces or to determine wear mechanisms. Several different carbon seal ring materials were used in the study, including two carbon composites now under development at United Technologies Research Laboratories.

	440C Stainless Steel	Beryllium Copper	52100 Bearing Steel
Rockwell Hardness	R_C58	R_C38	R_C62
Modulus of Elasticity (GPa)	200	131	207
Thermal Conductivity (W/m·K)	24.2	100.5	38.1
Coefficient of Thermal Expansion (10^{-6}/°C)	100.8	167.4	126.2

TABLE 1 Properties of metallic ring materials used in this study

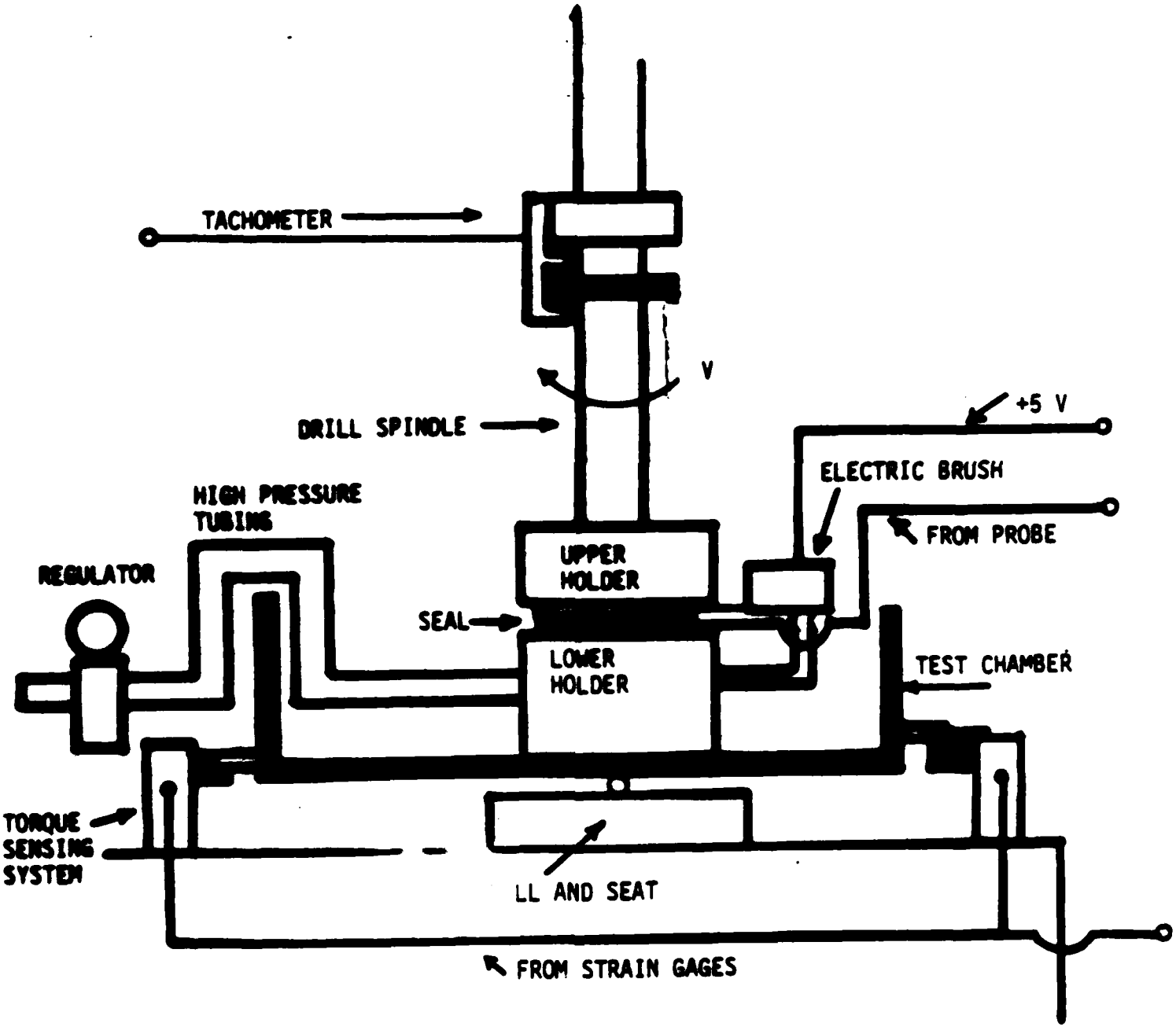

FIGURE 1. SCHEMATIC DIAGRAM OF TEST APPARATUS

Experimental/Numerical Technique for Stress and Temperature Analysis

In some of the dry tests, more information was required about contact conditions than could be determined with certainty from the contact probe/thermocouple device. For example, although the shape of the surface temperature profile determined by the dynamic thermocouple was considered to be reasonably accurate, some doubts remained about the accuracy of the temperature magnitudes. (The thermocouple was calibrated statically at two temperatures, 0°C and 100°C.) The contact pressure distribution was also desired and, in some cases, so was the stress distribution around the contact. To accomplish those tasks, the probe/thermocouple was used, along with finite element temperature and stress analysis programs, in a combined experimental/numerical technique. The technique was as follows: The contact probe was used in the patch location mode to find and characterize the geometry of contact patches in an operating face seal. The probe was then switched to the dynamic thermocouple mode to determine the face temperature within the patches. Static thermocouples were used at the same time to determine temperatures at the rear (non-contacting) faces of the seal rings.

To verify the temperature magnitudes and to determine stress distribution, thermal and stress analysis was carried out using finite element methods. A finite element model of a single contact was generated, based on the measured geometry of the rings and of a single contact patch. The thermal analysis used a surface temperature analysis program [7,8] which has recently been modified to enable more accurate solution of the convective diffusion problem encountered in sliding contacts with frictional heating [2]. Boundary conditions for the thermal analysis included the measured rear face temperatures and an assumed uniform heat flux in the contact patch, determined from measured friction force and velocity data. The predicted surface temperature profile was compared with that measured with the dynamic thermocouple. Adjustments were made in the

assumed heat flux distribution, while keeping the total heat flux constant, to produce a surface temperature profile in agreement with the experimentally-determined profile. This procedure enabled determination of both the temperature distribution in the vicinity of the contact patch and the distribution of frictional heat at the patch interface. From the latter could be found the contact pressure distribution. Using the contact pressure along with the friction coefficient and the temperature distribution, the deformation and stress distributions around the contact patches were then determined in a finite element thermoelasticity analysis.

Profilometry Apparatus

Profiles of the seal ring surfaces have been obtained using profilometry equipment purchased with ONR support. The heart of the system is a Bendix Linear Proficorder which enables surface roughness and waviness determination for a variety of geometries. To enable seal ring topography to be measured, an Alpha-Round high accuracy, motor driven, air bearing rotary table is used to rotate the ring-shaped specimens beneath the Proficorder's stationary tracer head. A fixture was built to accurately locate and level the seal ring on the rotary table.

As with most commercially-available profilometers, the Bendix instrument uses analog electronics to determine the most basic surface information (roughness average) and to plot the surface profile. In order to characterize the surface topography more completely, digital acquisition and analysis of the topographic data are necessary. Consequently, we have been devoting considerable effort to the computerization of the surface profilometry system. A dedicated microcomputer has been developed for acquiring the profile data from the Proficorder, doing preliminary analysis of the data, and storing it on a diskette for later analysis.

The operation of the system is as follows: The program is initialized from a terminal residing at the system. The user is asked to input variables required for evaluation of the data that are to be collected (What sampling rate? etc.). When the system has been initialized, gathering of surface data can commence. The microcomputer orders an analog to digital converter (ADC) to make a conversion. The ADC signals that the conversion is completed. The data are put in buffer memory in the microcomputer for later transferral to storage on the diskette. The interrupt timer residing on the microcomputer board is programmed to give the desired sampling rate. Once all the samples are taken, processing of the data will begin.

The data are corrected to eliminate tilt of the measured surface. This is done by Fourier analysis for a circular trace. These corrected data are then stored on the diskette.

When the operator wants to perform the numerical processing, he inserts the diskette and asks the microcomputer system to pass the file to a mainframe computer which has the computational power to perform some otherwise very time-consuming calculations such as the Fast Fourier Transform. The operator can choose what surface roughness parameters and distributions he wants to have calculated and whether he wants them displayed on a terminal or on a printer. The parameters and curves that will be available include: center-line, peak to valley height, ten-point height, center-line average, root-mean-square roughness, average radius of curvature of peaks, standard deviation of radius of curvature of peaks, average slope, standard deviation of slopes, number of peaks per unit length, height distribution histogram, the Abbott curve, skewness, kurtosis, auto-correlation function, wavelength, and power spectral density function. Up to the present time, the only topographic information of real interest in the seal ring study has been the location and relative height of the waviness peaks on the metallic seal ring surface. Thus the detailed

data analysis described in the last paragraph has not been necessary yet and is, in fact, still under development. It will be used extensively in the next phase of this research - the study of ring wear and its relationship to and effect on topography.

RESULTS AND DISCUSSION

Contact Probe Results - Dry Tests

A series of tests was performed using the three different metallic ring materials rotating at velocities ranging from 62.8 rad/s to 188.5 rad/s. Before all tests the metallic rings were lapped and polished to a surface roughness of 0.1 μm Ra or less. The stationary carbon ring was cleaned and, if necessary, lapped to insure that its embedded contact probe was working. A normal load of between 65 N and 90 N was applied to the seal before rotation at the desired velocity was begun.

In all cases, regardless of the rotor ring material or the sliding velocity, the contact probe showed evidence of small, distinct contact patches being present as soon as seal rotation began. The 5 volt pulses produced by the contact patches were approximately stationary on the oscilloscope screen. Since the oscilloscope trace was triggered at the same point on the rotating metallic ring each revolution, this showed that the patches were fixed locations on the metallic ring surface and were rotating with that ring.

A typical contact probe output trace, taken about 10 minutes after the beginning of a test, is shown in Figure 2. The test had a rotating seal ring of 440 C stainless steel in contact with a carbon graphite stationary ring at a rotary speed of 125.7 rad/s (1200 rpm). Two distinct contact patches are present on the metallic ring surface, one slightly larger than the other and both together making up a total of about 15% of the ring circumference. The surface temperature within the patches appeared to be between 120 and 190°C, with an increase toward the trailing edge (at left in Figure 2) and with the smaller patch being slightly hotter than the larger one.

In most cases the contact patches began to grow soon after the test began, both by enlargement of the patches and by the formation and joining together of new contact spots. This behavior is shown in Figure 3, which shows a sequence

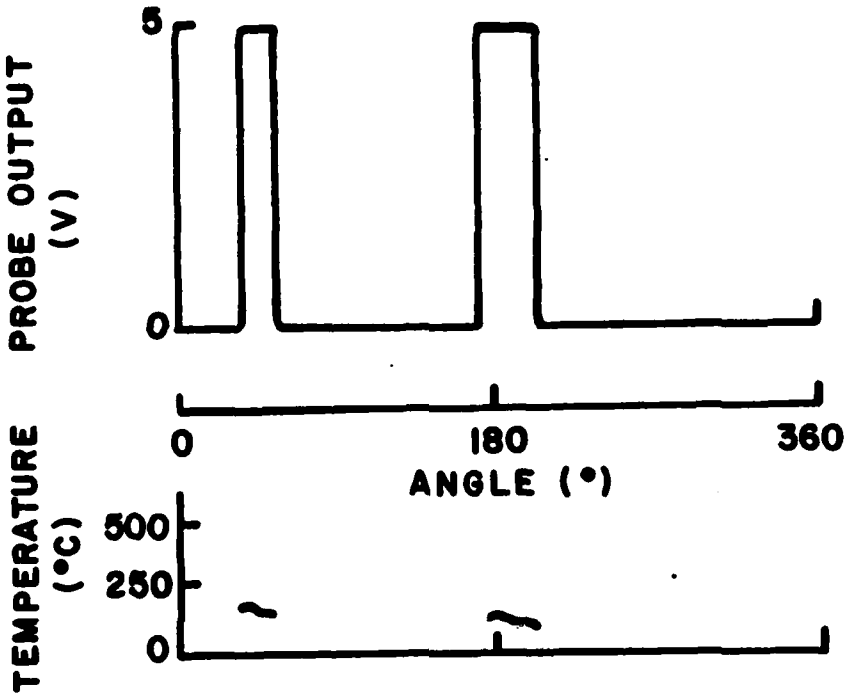

FIGURE 2. CONTACT PROBE OUTPUT (above) AND DYNAMIC THERMOCOUPLE OUTPUT (below) DURING TEST WITH 440 C STAINLESS STEEL SEAL RING ROTATING AT 125.7 RAD/SEC UNDER DRY CONDITIONS.

of contact probe traces obtained during a test at 125.7 rad/s with a beryllium copper rotating ring. Immediately after the test began, two small contact spots were detected, with their surface temperature being about 135° - 155°C. Soon thereafter a third patch of contact formed and then the patches slowly enlarged, with their temperatures decreasing. After about fifteen minutes of operation, four distinct patches were observed and a fifth was just beginning. The surface temperatures had decreased to about 115° to 125°. Later, after about 45 minutes of testing, the patches had enlarged and joined together, producing two patches, together making up about 80% of the ring circumference.

Considerable differences were found between the results at different velocities and with different metallic ring materials. Most of those results are reported elsewhere [11,12]. Although the results showed that there is no unique set of contact patch characteristics associated with any set of test parameters, there are some significant trends and they may be summarized as follows:

- Contact patches observed with beryllium copper rotating rings tend to be larger and at a lower temperature than those with either 440 C stainless steel or 52100 bearing steel rings. The 52100 rings tended to have the smallest and hottest contact patches.
- With a given metallic ring material, contact patches tend to be larger and cooler at lower sliding speeds. Complete contact over the ring circumference is achieved at low velocity, with the critical velocity for patch formation being a function of material properties. (Beryllium copper had the highest critical velocity of the three materials tested, and 52100 bearing steel, the lowest.)
- The friction coefficient, f, was approximately the same for all materials and at all velocities ($f = 0.12 \pm 0.02$).

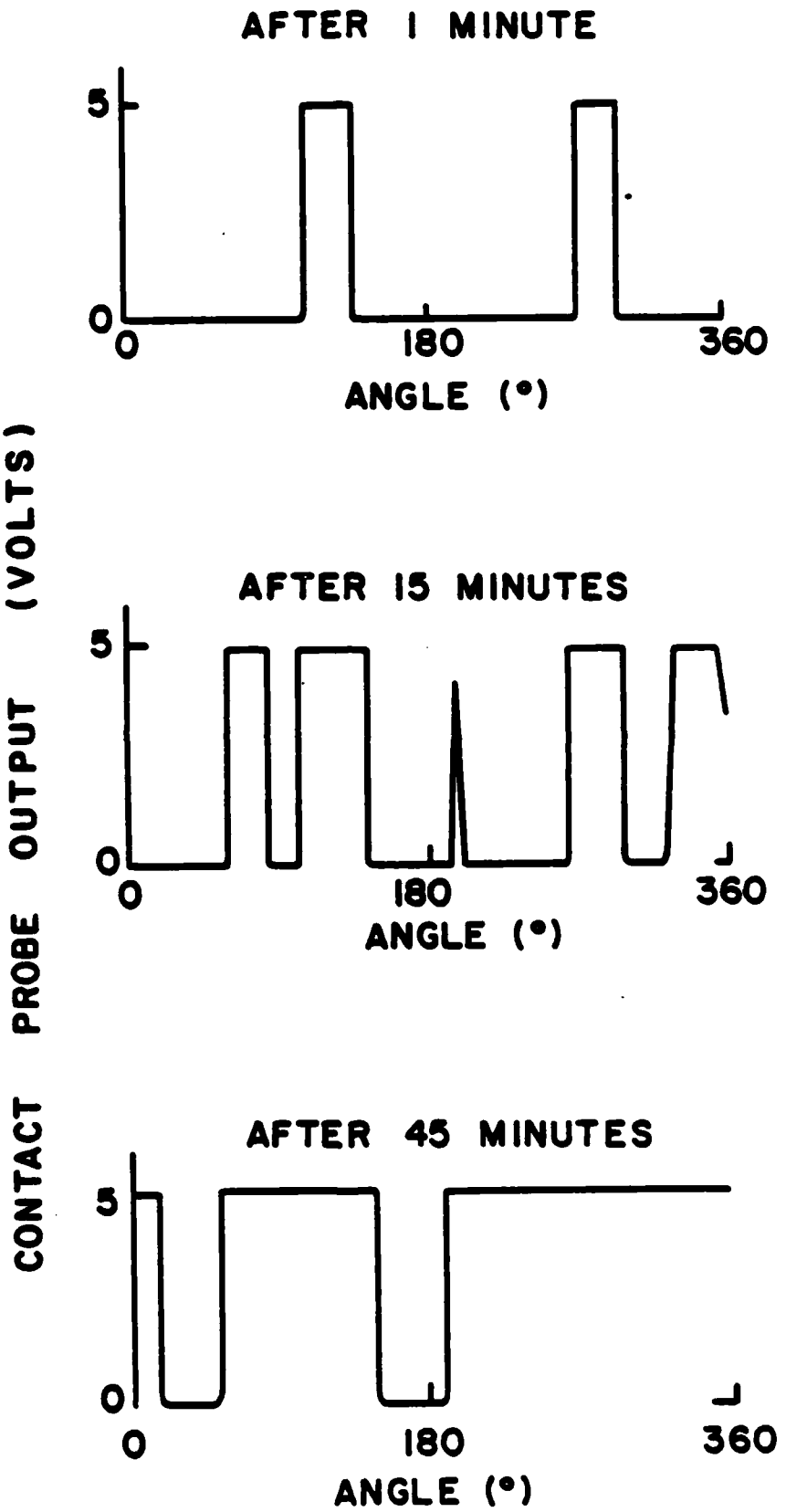

FIGURE 3. SEQUENCE OF OUTPUT TRACES FROM CONTACT PROBE, SHOWING GROWTH OF CONTACT PATCHES ON ROTATING BERYLLIUM COPPER RING (125.7 rad/s, dry operation)

Based on these results, and using the material properties given in Table 1, it appears that the seal ring materials least susceptible to the formation of a few small, hot, long-lasting contact patches are those with high thermal conductivity and low wear resistance. A combination of heat conduction (away from the patch) and wear can lead to the enlargement of the contact patches, resulting in more uniform contact and lower contact temperatures. Lower velocities also result in more uniform contact (larger contact patches) and lower contact temperatures. These parametric influences are similar to those predicted by Burton and his co-workers [3,13]. The contact patch lengths are much larger than those predicted by that earlier work, however [12].

Some tests were run with the carbon graphite ring as the rotating ring and with the contact probe mounted in the stationary 440°C stainless steel ring. The results for those tests strongly indicate that the contact patches tend to develop on, and remain stationary with respect to, the metallic ring. In general, either there was complete contact at the probe location throughout the test, or there was no contact throughout the test. In one test, for example, at 188.5 rad/s, continuous contact was noted at the contact probe throughout the testing period. Disassembly of the seal showed evidence of contact and wear at the probe location, demonstrating that a contact spot had been centered there. The seal was then reassembled, without the usual preliminary polishing, and tested again under the same conditions. The test showed no contact at the probe. Evidently the wear at the initial patch location was sufficient to cause a small depression to form after the ring cooled. Upon further operation the contact patches were located at new, higher positions.

Contact Pressure and Temperature Analysis

In the study of contact pressure and temperature distribution it was decided to concentrate on one pair of seal materials, 440 C stainless steel vs

carbon graphite, one velocity, 125.7 rad/s, and one normal load, 90 N. In order to obtain boundary conditions for the surface temperature analysis, two static thermocouples were used. One was mounted on the rear (non-contacting face of the stationary carbon graphite seal ring and was monitored continuously during the 15 minute test. The other was applied to the rear face of the metallic ring immediately after the test machine was shut off and rotation stopped. Otherwise, the test was run as described earlier and both contact probe and dynamic thermocouple were used to characterize the patches. In fact, the results are those shown in Figure 2.

The dynamic thermocouple indicated that surface temperatures in each of the two contact patches reached a peak near the trailing edge. Temperatures ranging from 110-120°C to 180-190°C were measured within the contacts, but these values are not considered exact. The thermocouple output signal was rather noisy, making accurate reading quite difficult, and the calibration, which was done statically at 0°C and 100°C, may not be completely valid under dynamic sliding conditions at higher temperatures. The doubts about the accuracy of the temperature magnitudes did not carry over to the shape of the surface temperature profile. Earlier results had shown a similar general increase in temperature from leading to trailing edge [12].

To verify the temperature magnitudes, a thermal analysis was done using a recently developed finite element program [7,8]. The model was of a segment of the seal rings stretching from one mid-section between the two patches to the next mid-section, and including one complete contact patch. The geometry of the seal rings and the measured contact patch length (8.5 mm) were used in generating the finite element mesh which is shown in Figure 4. Boundary conditions, based on the test results, were fixed temperatures 84°C and 88°C on the rear faces of the carbon and stainless steel rings, respectively. The conditions encountered by the two contact patches were assumed to be identical, so the

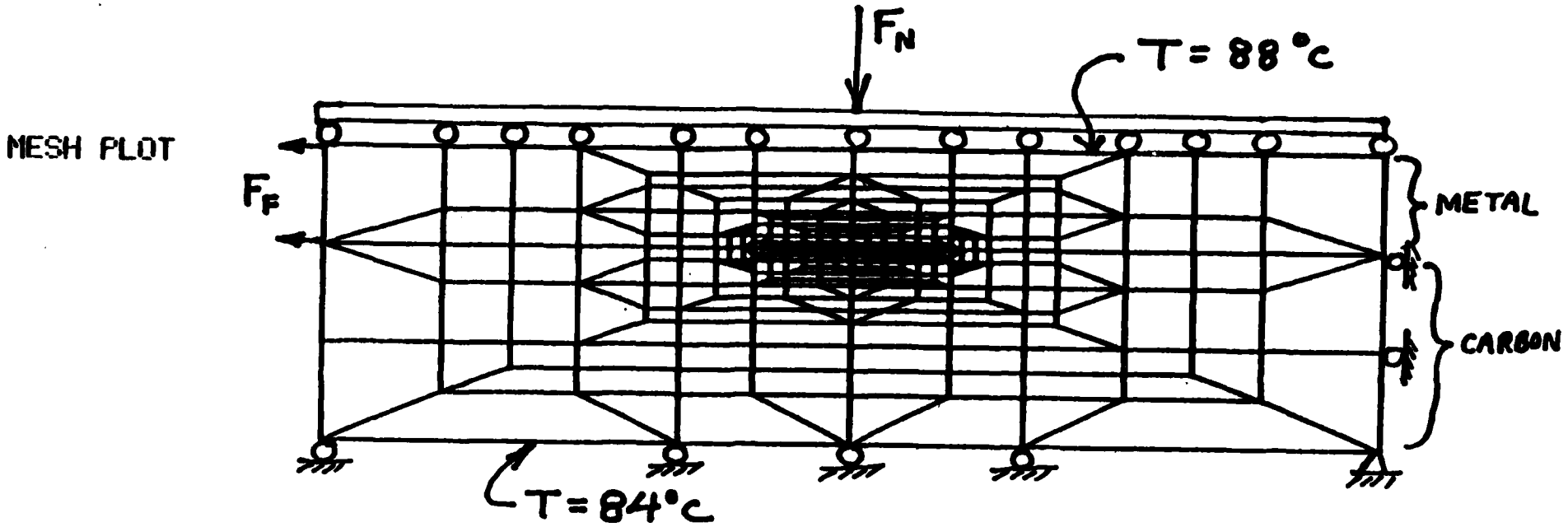

FIGURE 4. FINITE ELEMENT MESH FOR SEAL THERMAL AND STRESS ANALYSIS

nodes at the left end of the mesh were assumed to be at the same temperature as those at the right end. The total frictional heat loss, determined from the friction force and velocity data, was assumed to be equally shared by the two patches and was initially assumed to be distributed uniformly along the patch.

The temperature distribution predicted using the above conditions had a temperature peak located between the center of contact and the trailing edge, but closer to the center than was noted experimentally. This was attributed to a mistaken assumption of uniform heat flux distribution. In reality the heat flux distribution within the contact must follow the contact pressure distribution, assuming a constant coefficient of friction. To determine the contact pressure distribution a thermoelasticity analysis was performed using the FEATS finite element program. The finite element mesh was the same as that used in the thermal analysis (Fig. 4) and the boundary conditions are also shown in Fig. 4. Half of the measured friction force and normal force were applied to the seal segment, and the temperature distribution from the thermal analysis was used. The resulting contact pressure distribution (distribution of axial stress in contacting elements) was non-uniform, with a peak near the trailing edge. This was then used to adjust the distribution, but not the total, of the frictional heat flux at the contact interface and a new thermal analysis was performed. The new temperature distribution was used in the stress analysis program to obtain a new contact pressure distribution. This second contact pressure distribution was very similar to the first, so the iterative calculation procedure was stopped at this point.

The resulting surface temperature and contact pressure distributions are shown in Figs. 5 and 6, respectively. Both exhibit peaks near the trailing edge of the contact patch. The surface temperature profile is very similar in shape to that measured experimentally (Fig. 2), although the direction of motion is different in the two Figures. The magnitude of the measured temperatures (Fig.2)

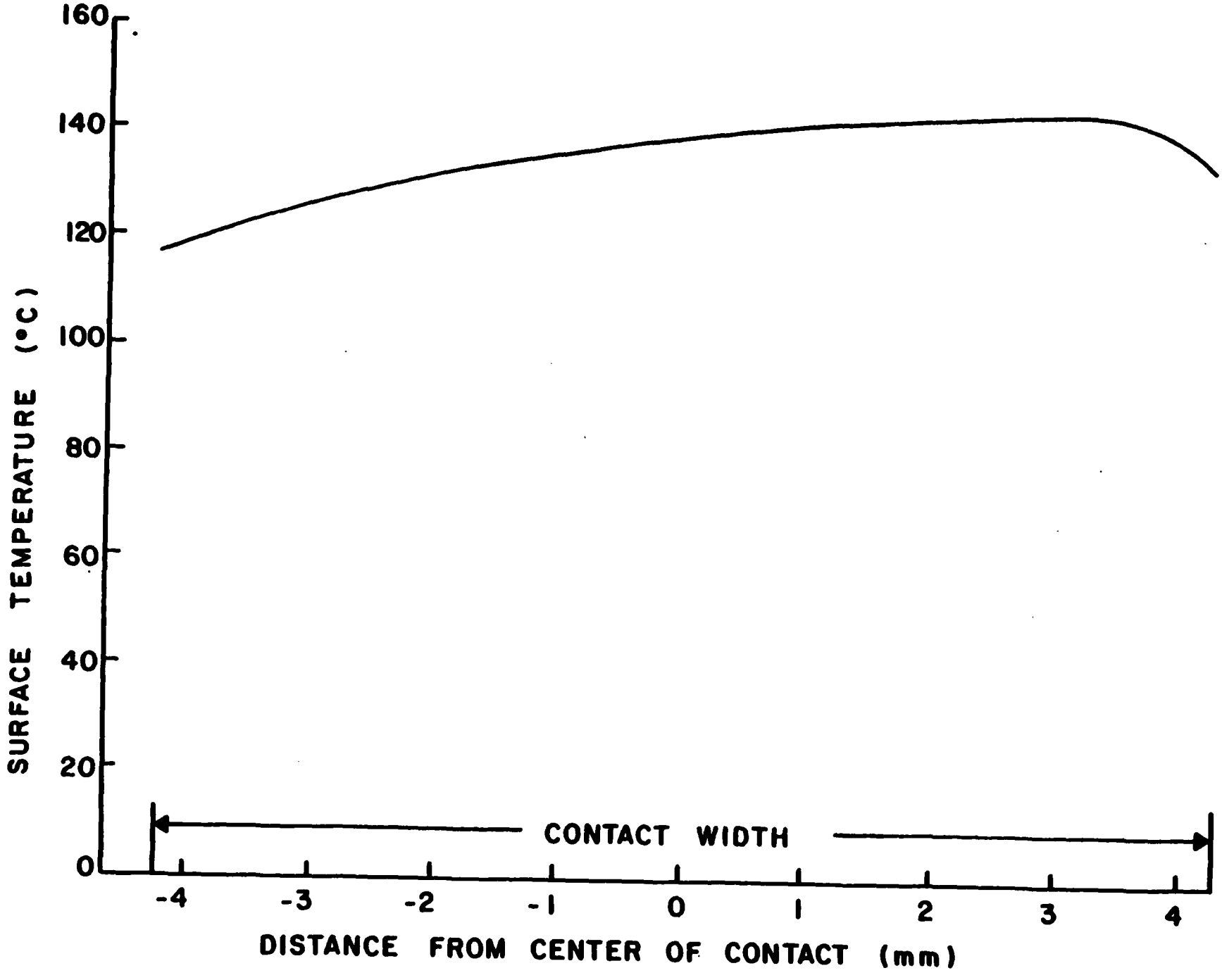

FIGURE 5. SURFACE TEMPERATURE DISTRIBUTION WITHIN CONTACT PATCH

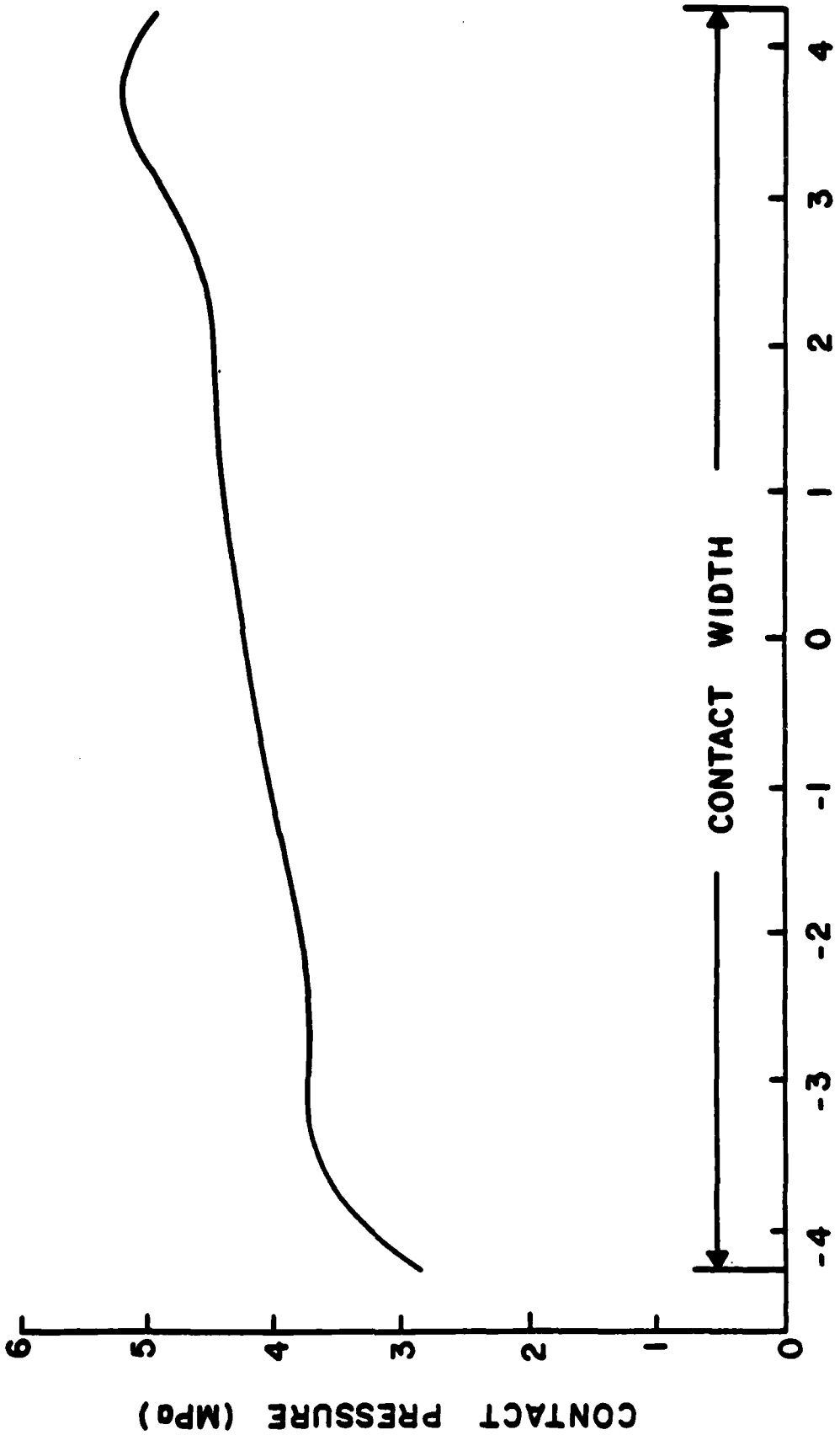

FIGURE 6. CONTACT PRESSURE DISTRIBUTION WITHIN PATCH

appears to be about 15% higher than those determined analytically. Most of this difference may be attributed to inaccuracies in the dynamic thermocouple measurements.

Stress Distribution

The stress analysis showed that thermal stresses and deformation are more important than those caused by mechanical loading. In most locations near the contact patch the stresses and deformations due to the combined thermal and mechanical loadings were at least an order of magnitude higher than those due to mechanical loadings alone. This is in agreement with stress analyses of hypothetical contacts done recently by other researchers [14].

The largest equivalent stress values occur in the region of highest temperature. This can be seen in Figures 7 and 8. Both Figures focus on a region around the contact patches, with Figure 7 showing isotherms in that region and Figure 8 showing isobars (lines of constant equivalent stress). From Figure 7 it can be seen that temperature gradients are a bit more severe in the carbon ring, with respect to which the heat source is moving. In contrast, the stresses in the metallic ring are much larger (by almost an order of magnitude) than the stresses in the carbon. This difference, which is due to the difference in elastic moduli between the two materials, accounts for the fact that no high stress isobars are seen in the carbon ring in Figure 8. The largest equivalent stresses occur very close to the point of peak surface temperature in the metallic ring. Although the peak stresses in this case, about 75 MPa, were not large enough to cause plastic deformation, it is expected that the peak stress in more concentrated, hotter contacts could easily exceed the yield stress of the metallic ring material.

A study of the stress analysis results showed that the largest principal stresses in the region around the contact patch, at least in the metallic ring,

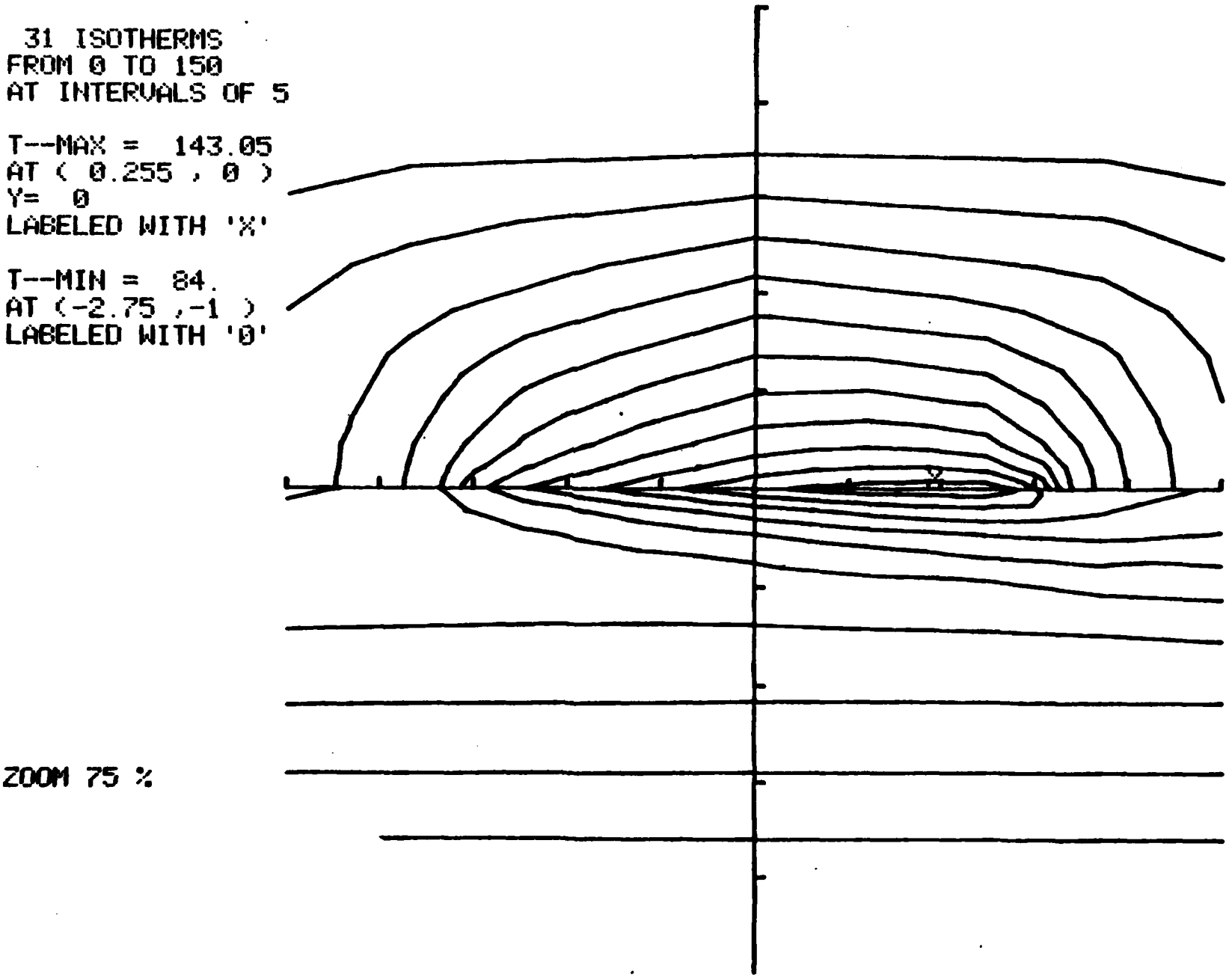

FIGURE 7. ISOTHERMS IN CONTACT REGIONS. MAXIMUM TEMPERATURE (144°C) LOCATION GIVEN BY X. ISOTHERMS EVERY 5°C.

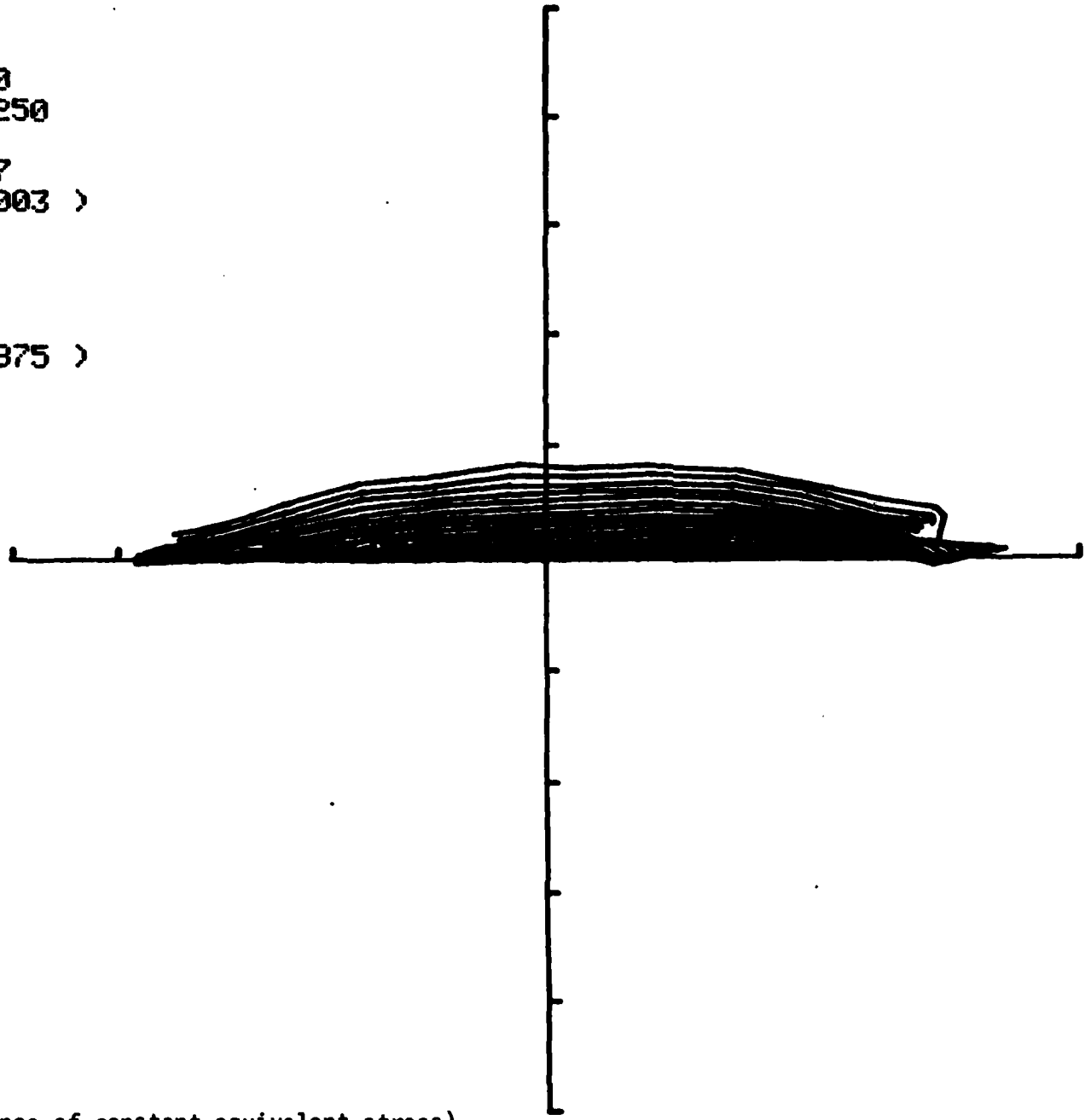

FIGURE 8. ISOBARS (lines of constant equivalent stress) IN REGION OF CONTACT PATCH. ISOBARS PLOTTED FROM $\bar{\sigma}$ = 35 MPa to $\bar{\sigma}$ = 76.02 MPa ($=\bar{\sigma}_{max}$) at intervals of 2.5 MPa.

are all compressive. This is attributed to the dominance of thermal deformation in that region. Such a state of stress cannot directly cause cracks to be initiated. The only plausible explanation for the occurrence of thermocracks on the surface of metallic seal rings is that they are caused by residual stress. If the temperatures in a contact patch are high enough, significant thermal stress would occur in that region. The thermal stress, which is predominantly compressive, could cause substantial plastic deformation in that region. If the contact patch then moved elsewhere, owing to either wear or cooling, there would be a resulting residual tensile stress in the plastically deformed region. The residual stress could cause cracking of the seal ring material in that location. This proposed thermocracking mechanism has been shown to be consistent with observed microscopic observations of thermocracked seal rings [6].

Relationship Between Surface Profile and Contact Patch Location

When the first measurements were made of contact patch sizes and locations [11], it was hypothesized that the contacts were located at waviness peaks on the contact surface of the metallic ring. We were at the time unable to verify that hypothesis. Recently, with the acquisition of the profilometry systems described above, we have been able to start addressing that question and determine the relationship between contact patch locations and ring surface profiles.

Mechanical face seals are typically lapped to a high degree of flatness before operation. Despite this, seals always have some initial waviness present on their surface and this waviness has been observed to grow during seal operation [15]. In our work we have attempted to lap our seals to industry specifications prior to testing. Yet, in all cases, solid/solid contact was found to occur at discrete patches on the seal interface. There was distinct evidence of wear and carbon transfer at locations on the metallic seal surface which corresponded closely with measured patch locations [2,12]. In order to relate those patch locations to the surface profile of the metallic ring, several metallic rings had their surface profile determined after testing and the profile was compared with the contact probe measurements of contact patch locations.

A typical contact probe output trace is shown in Figure 9. The trace is from a dry test of a carbon graphite stationary ring in contact with a 440 C stainless steel ring. The photo was taken after about 15 minutes of testing at 125.7 rad/sec. Three distinct contact patches are seen, with some evidence of a fourth forming (at about 40° from starting point). Soon after the photo was taken the seal was disassembled and the surface profile of the metallic ring was measured. The ring was rotated beneath the profilometer's measuring head on an accurate air bearing rotary table. The resulting profilometric data were

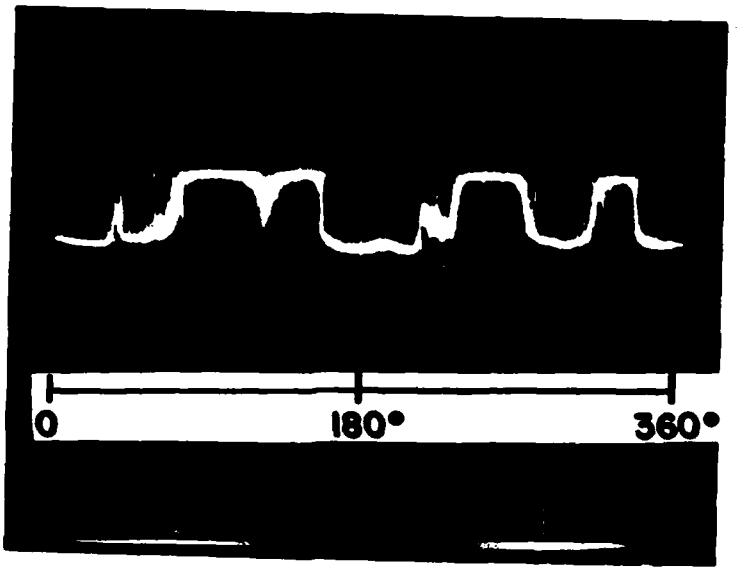

FIGURE 9 Contact probe output after 16 minutes of dry test of rotating 440C stainless steel ring vs. stationary carbon graphite ring at 125.7 rad/sec.

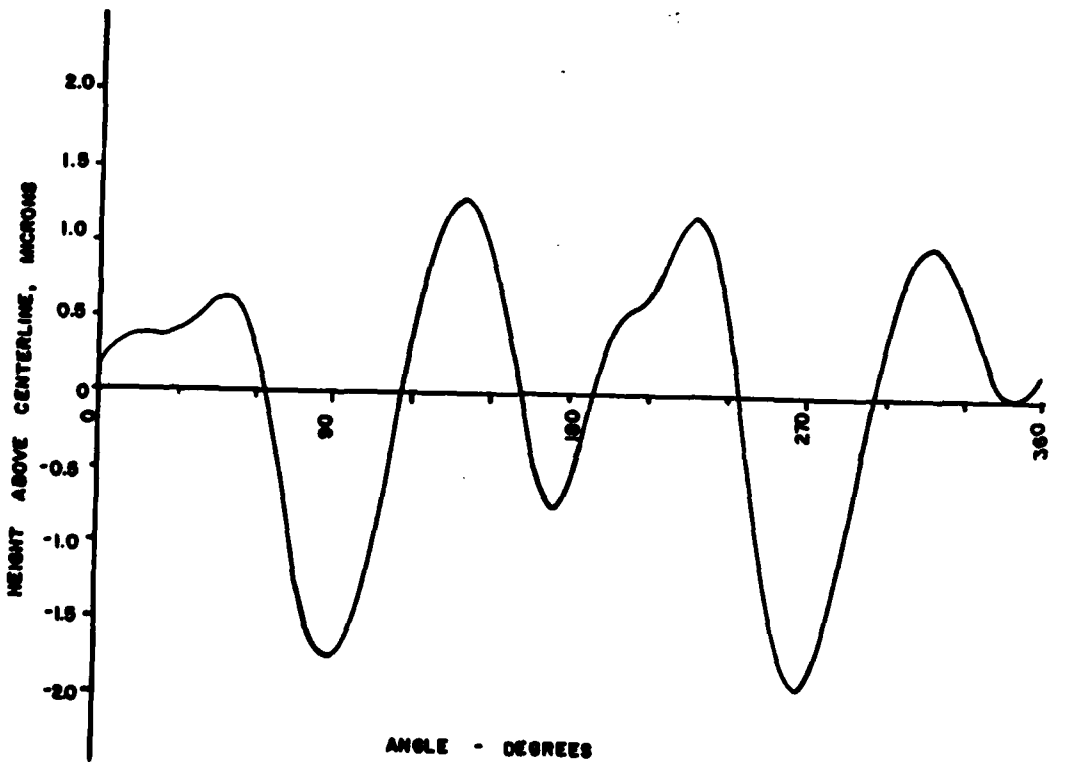

FIGURE 10 Surface profile of metallic ring after test of Figure 9.

then preprocessed by analysis software which subtracted ring tilt (by doing a Fourier analysis of the data and subtracting the first harmonic) and then subtracting the centerline of the remaining height distribution. A plot of the preprocessed profile data is shown in Figure 10. It can be seen that the metallic ring has a waviness which has four distinct peaks around the ring circumference. Three of the peaks are higher than the fourth and the locations of those peaks are the same as those of the three measured contact patches. The highest of the peaks, located at about 140°, appears to be at the beginning of the broadest contact patch. The smallest peak is at about the same location as the small patch just coming into contact in Figure 9.

The results shown in Figure 9 and 10 are similar to that obtained in other tests with both 440 C and 52100 rotating rings under both dry and liquid lubricated conditions. Thus, there is strong evidence to support the hypothesis that contact patch locations coincide with peaks of the surface profile waves. There is also evidence to indicate that wear occurs at those peaks to change the surface profile and to cause movement of the contact patches. Some such wear is evident in Figure 10, particularly at the first and third peaks. The worn shoulder of the third waviness peak is also seen in Figure 9 to be a location of light contact adjacent to a contact patch which is located at the higher portions of that peak. Further work is now in progress to study the progression of that wear and the factors that affect it.

Wear Results

Wear data were gathered during some of the dry tests of seal rings. Before each of these tests both metallic and non-metallic seal rings were lapped and then ultrasonically cleaned and weighed on an accurate analytical balance. After installation of the rings a normal force of 92 N was applied to the seal and the rotating ring was set in motion at a preset velocity. The tests continued

for 1 hour, after which the seal was disassembled. Each ring was then again cleaned and weighed. Wear was therefore determined as the total weight (or mass) lost during the 1 hour test.

Three different carbon ring materials were tested in this series of tests; the commercial carbon graphite material (Pure Carbon grade P658RC), and graphite fiber-glass matrix composite materials (Compglas™) produced by United Technologies Corp. Research Center. One of the carbon composites contained 40% carbon fiber and the other 45%. All carbon rings were run against a 440 C stainless steel rotating ring.

Results of the series of tests are presented in Table 2. All of the data are averages of two or more runs. From the data it can be seen that the carbon-glass composite materials wore much less than the carbon graphite ring under the same conditions but those rings caused slightly more wear on the stainless steel ring. The carbon composite ring containing the least (40%) carbon fiber experienced the least wear but wore the metallic ring the most. In all cases it was found that a decrease in wear of the carbon ring was accompanied by an increase in metallic ring wear.

From the last two entries in Table 2 it can be seen that a decrease in surface velocity (and total sliding distance) by 33% resulted in a decrease in wear of the metallic ring by about 33% but a much smaller relative decrease (20%) in carbon ring wear. That appears to indicate that the carbon ring wear rate (wear per unit sliding distance) was not constant, but was greater earlier in the run. Further tests are underway with all material combinations to verify this conclusion and to ascertain where on the ring surfaces the wear occurs.

TABLE 2

Results of Wear Tests of Seal Rings

Test Combination	Surface Velocity m/s	Carbon Ring Material	Carbon Ring Wear (mg)	Metallic Ring* Wear (mg)
1	4.95	carbon graphite	59.8	2.1
2	4.95	carbon-glass (45% C)	20.6	6.6
3	4.95	carbon-glass (40% C)	40.5	3.7
4	3.3	carbon-glass (40% C)	32.4	2.5

*440 C stainless steel metallic ring in all cases

Test duration for all tests: 1 hour

Normal force for all tests: 92 N

All tests were run dry (no sealed liquid)

Contact Probe Results - Liquid Lubricated Tests

In the liquid lubricated seal tests, pressurized water was introduced as a sealed fluid at the interior of the seal. The tests were then run using the same procedure described earlier for the dry tests. Previous results with liquid lubricated seals [12] had shown that the contact probe signal tended to be shorted through the thin film of sealed liquid between the seal faces. In these tests some of the same current leakage occurred but, owing to careful test procedures, a lower fluid pressure, a larger normal force between the seal faces, and some electronic signal filtering, the contact probe and thermocouple both gave clear indications in most cases.

Many of the results of the liquid lubricated tests were similar to those described earlier for dry tests. A typical set of results is shown in Figure 11 for the case of carbon graphite stationary ring and beryllium copper rotating ring. In Figure 11a is shown a photo of the contact probe output at the beginning of a test at 62.8 rad/sec angular velocity. Despite lapping of the rings prior to the test there is evidence of five distinct contact patches, comprising a total of about 25% of the ring circumference. The temperature in the patches is 85-90°C, according to the dynamic thermocouple output. Later, after about 3 minutes of testing the patches had grown and merged into three large patches, making up nearly 75% of the circumference and having temperatures ranging from 55-60°C (Fig. 11b). Still later, after 7 minutes of testing, there was a shrinkage of the patches that seemed to be accompanied by (or related to) leakage of fluid from the seal. These patches gradually grew until after about 15 minutes there were again three large contacts similar in size to those in Figure 11b.

At higher speeds there tended to be smaller contact patches, as was the case with dry operation. Figure 12a and b show results for beryllium copper

rings rotating at 125.7 and 188.5 rad/sec respectively. The photos show contact probe output after about 30 minutes of operation, when the patch size had settled to a steady size. It can be seen that the total patch length was shortest for the 188.5 rad/sec test (≈ 35% of the ring circumference) and was larger (about 50%) for the 125.7 rad/sec tests. As was shown in Figures 11, the contact patches covered a total of about 75% of the ring circumference in the 62.8 rad/sec tests. Thus, as was found earlier in the dry tests [11], the contact patch length decreases as the speed increases. The surface temperature within the patches was also found to be higher for shorter patch lengths in these liquid lubricated tests (up to about 150°C for the 188.5 rad/sec tests). These temperatures were somewhat lower than those measured in dry tests under the same conditions [11], although the friction coefficient was nearly the same as that measured in the dry tests (f = .15). An analysis of the surface temperatures indicated that the major reason for the lower temperatures was transfer of heat to the sealed fluid at the inside of the rotating seal ring.

Tests with 440 C stainless steel mating rings showed the same trend as that observed in the beryllium copper tests. There were fewer, larger, and cooler contact patches at lower speeds than at higher velocity. The same tendency was noted with 52100 bearing steel mating rings. These results are similar to those found earlier in dry tests of those materials.

One result of the liquid lubricated tests that differed from those of the dry tests was a slight tendency of the friction coefficient to be lower at higher velocities, particularly with the 440 C mating rings. The average friction coefficient was .15 at 62.8 rev/sec, decreasing to .13 at 188.5 rev/sec. This could be an indication of more effective hydrodynamic lubrication at higher velocities. Another difference between the wet and dry tests was the more stable nature of the contact patches in the dry cases. As noted above, there were more sudden changes in patch size in the liquid lubricated tests than had been observed in dry cases.

FIGURES 11. Contact probe output during test at 62.8 rad/sec of rotating beryllium copper ring vs. stationary carbon graphite ring with pressurized water as sealed fluid.

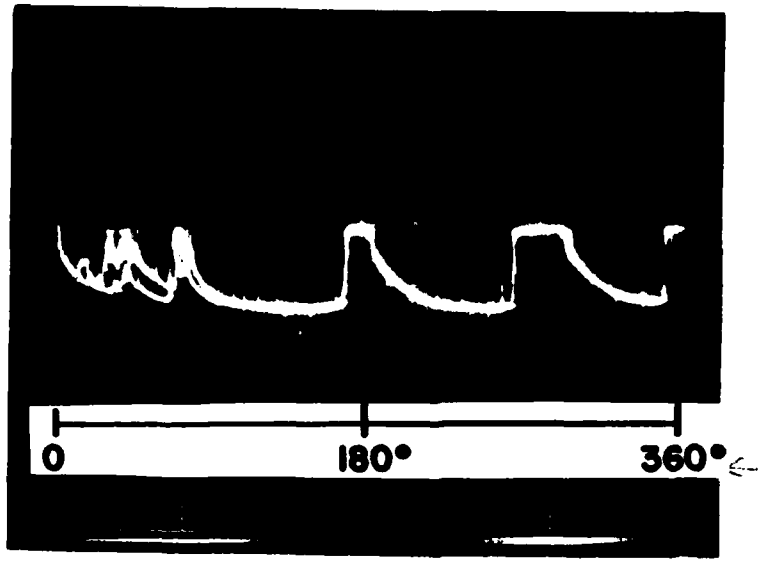

FIGURE 11a. Immediately after commencement of test

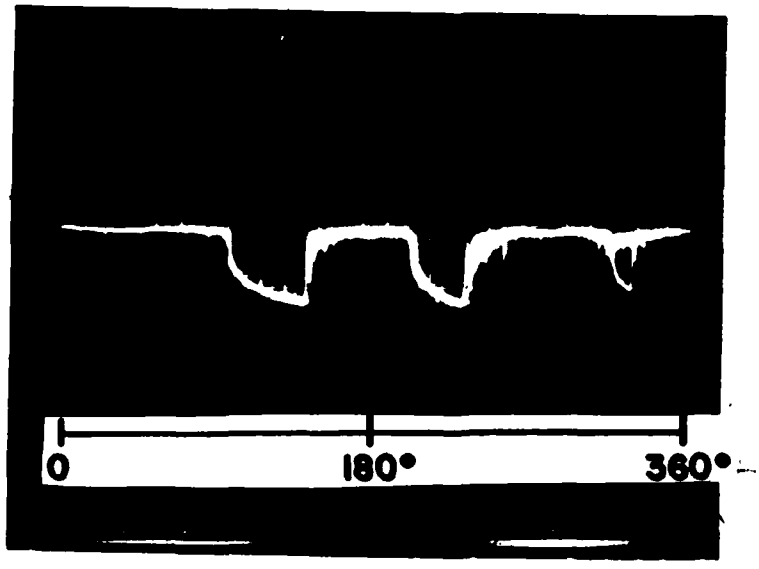

FIGURE 11b. After 3 minutes.

FIGURES 12. Contact probe output near end of tests of rotating beryllium copper ring vs. stationary carbon graphite ring with pressurized water as sealed fluid.

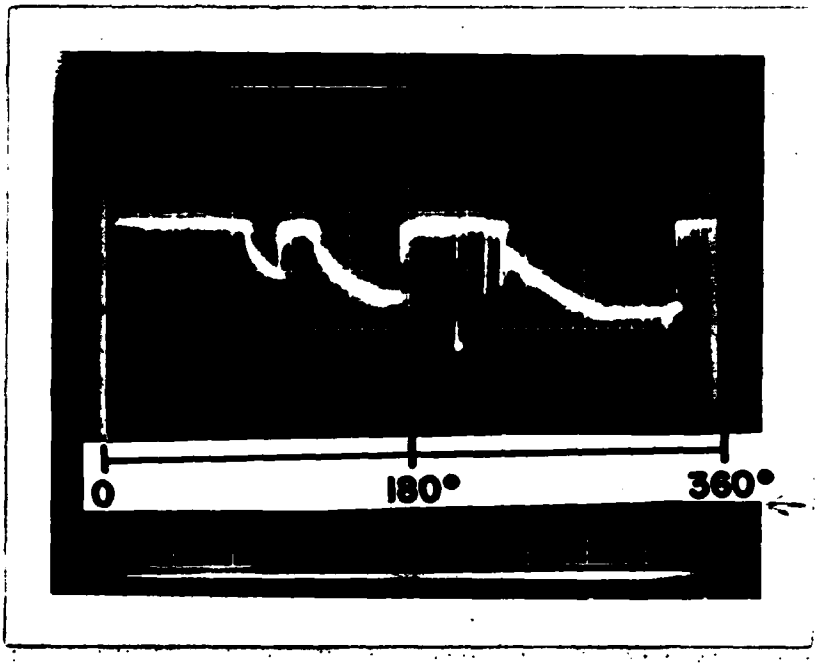

FIGURE 12a. 125.7 rad/sec

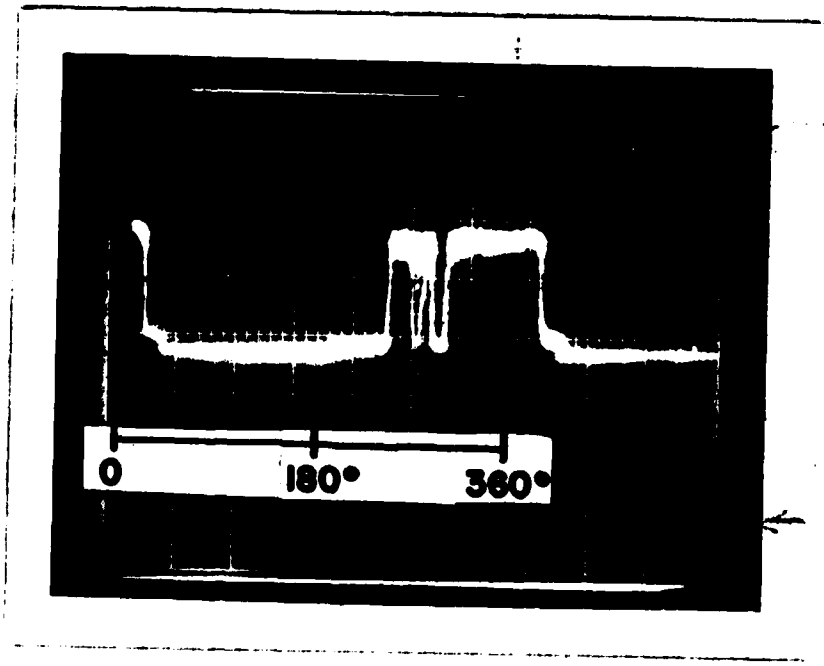

FIGURE 12b. 188.5 rad/sec

CONCLUSIONS

It was found that contact in face seals is concentrated in several (2-5) small patches distributed around the seal interface. In a carbon graphite/metallic face seal, the patches remain approximately stationary with respect to the metallic ring, whether that ring be stationary or rotating. This is true of both dry and liquid lubricated operation, although the contact patches were more transitory in nature in the liquid lubricated case. In both cases the patch length is smaller, and surface temperatures higher, at higher seal velocities and with less conductive or more wear resistant metallic rings. The peak surface temperature occurs near the trailing edge of the contact patch and the heat flux and contact pressure distributions within the patch also reach a peak near the trailing edge. The largest contribution to the stress distribution near the contact patches is thermal stress, with stresses caused by surface tractions being smaller in magnitude. The maximum stress near the small hot patches could be large enough to cause plastic deformation and this could be responsible for the thermocracks which occur in some seals.

The location of the contact patches was found to coincide with the peaks of waviness on the surface of the metallic ring. There was evidence of wear at those peaks, although that localized wear has not yet been quantified. Measurements of gross ring wear have been made, however, and they show significant wear of the carbon ring, with less wear of the metallic ring. An increase in the wear resistance of the carbon ring is accompanied by an increase in the wear of the metallic ring.

REFERENCES

1. Kennedy, F.E., Grim, J.N., and Glovsky, R.P., "Factors Influencing Thermomechanical Failure of Face Seals", ONR Interim Report No. 1, Contract No.N00014-81-0090, Dartmouth College, January 1982.

2. Kennedy, F.E., Grim, J.N., and Glovsky, R.P., "Factors Influencing Thermomechanical Failure of Face Seals II", ONR Interim Report No. 2, Contract No. N00014-81-0090, Dartmouth College, January 1983.

3. Burton, R.A., Nerlikar, V. and Kilaparti, S.R., "Thermoelastic Instability in a Seal-Like Configuration", Wear, 1973, 24, 177-188.

4. Lebeck, A.O., "Theory of Thermoelastic Instability of Rotating Rings in Sliding Contact with Wear", ASME j. Lub. Tech., 1976, 98, 277-285.

5. Banerjee, B.N. and Burton, R.A., "Experimental Studies on Thermoelastic Effect in Hydrodynamically Lubricated Face Seals", ASME J. Lub. Tech., 1979, 101, 275-282.

6. Kennedy, F.E. and Karpe, S.L., "Thermocracking of a Mechanical Face Seal", Wear, 1982, 79, 21-36.

7. Kennedy, F.E., "Surface Temperatures in Sliding Systems - A Finite Element Analysis", ASME Journal of Lubrication Technology, 1981, 103, 90-96.

8. Glovsky, R.P., "Development and Application of THERMAP", Master of Engineering Thesis, Dartmouth College, June 1982.

9. Dow, T.A. and Stockwell, R.D., "Experimental Verification of Thermo-Elastic Instabilities in Sliding Contact", ASME J. Lub. Tech., v.99 (1977), pp.359-364.

10. Netzel, J.P., "Observation of Thermoelastic Instability in Mechanical Face Seals", Wear, 1980, 59, 135-148.

11. Kennedy, F.E. and Grim, J.N., "Observation of Contact Conditions in Mechanical Face Seals", to appear in ASLE Transactions.

12. Grim, J.N., "Observation of Thermoelastic Instabilities in Mechanical Face Seals", Master of Engineering Thesis, Thayer School of Engineering, Dartmouth College, July 1982.

13. Kilaparti, S.R. and Burton, R.A., "Pressure Distribution for Patchlike Contact with Frictional Heating, Thermal Expansion, and Wear", ASME J. Lub. Tech., 1976, 98, 596-601.

14. Ju, F.D. and Huang, J.H., "Heat Checking in the Contact Zone of a Bearing Seal (A Two Dimensional Model of a Moving Asperity)", Wear, 1982, 79, 107-118.

15. Lebeck, A.O., "Mechanical Loading-A Primary Source of Waviness in Mechanical Face Seals", ASLE Trans., v.20 (1977), pp. 195-208.

References (continued)

16. Kennedy, F.E., Colin, F., Floquet, A., and Glovsky, R., "Improved Techniques for Finite Element Analysis of Surface Temperatures", presented at 10th Leeds-Lyon Symposium on Tribology, Lyon, France, September 1983.

17. Kennedy, F.E., Grim, J.N., and Chuah, C.K., "An Experimental/Numerical Study of Contact Phenomena in Mechanical Face Seals", presented at 10th Leeds-Lyon Symposium on Tribology, Lyon, France, September 1983.

431:AWR:fmm
13 Apr 1983

ONR Distribution List - Tribology

Government

	One copy except as noted
Materials Division (Code 431) Engineering Sciences Directorate Office of Naval Research 800 N. Quincy Street Arlington, VA 22217	2
Mechanics Division (Code 432) Engineering Sciences Directorate Office of Naval Research 800 N. Quincy Street Arlington, VA 22217	2
Defense Documentation Center Building 5, Cameron Station Alexandria, VA 22314	12
Technical Information Division Naval Research Laboratory 4555 Overlook Avenue SW Washington, DC 20375	6
Division of Weapons & Engineering U.S. Naval Academy Annapolis, MD 21402	
Comandant of the Marine Corps (Code LMM-3) Headquarters, U.S. Marine Corps Washington, DC 20380	
Office of Naval Research Attn: Code 100M 800 N. Quincy Street Arlington, VA 22217	
DTNSRDC Mr. R. G. Brown (Code 2382) Annapolis, MD 21402	
Air Force Wright Aeronautical Laboratories Wright-Patterson Air Force Base Attn: J. Dill, H. Jones, POSL WPAFB, OH 45433	

Naval Air Propulsion Center
A. J. D'Orazio, Code PE-72
Trenton, NJ 08628

DTNSRDC
Attn: Mr. Jim Dray (Code 2832)
Annapolis, MD 21402

Naval Sea Systems Command
Attn: Mr. Richard W. Graham, II
Code 56X43, Bldg. NC 4, Room 374
Washington, DC 20362

DTNSRDC
Attn: Mr. Al Harbage, Jr. (Code 2723)
Annapolis, MD 21402

Naval Sea Systems Command
Attn: Mr. Martin Kandl (Code 56X31)
Washington, DC 20362

David W. Taylor Naval Ship R&D Center
Attn: S. Karpe
Ship Materials Engineering Department
Annapolis, MD 21402

Army Materials and Mechanics Research Center
Attn: Dr. R. N. Katz
Watertown, MA 02172

Naval Air Engineering Center
Attn: L. Kociuba, Code 92A3
Lakehurst, NJ 08733

Naval Air Systems Command
Attn: AIR-4111C (CDR A. H. Robbins)
Washington, DC 20361

Army Research Office
Attn: Dr. George Mayer
P.O. Box 12211
Research Triangle Park, NC 27709

Army Mobility Equipment R&D Command
Attn: M. LePera (DTDME-VF)
Fort Belvoir, VA 22060

Army Research Office
Attn: Dr. Fred Schmiedeshoff
P.O. Box 12211
Research Triangle Park, NC 27709

Air Force Wright Aeronautical Laboratories
Wright-Patterson Air Force Base
Attn: B. D. McConnell - MLBT
WPAFB, OH 45433

U. S. Army MERDC
Attn: W. McGovern
Fort Belvoir, VA 22060

Naval Air Development Center
Attn: D. V. Minuti (Code 606B)
Warminster, PA 18974

Naval Research Laboratory
Attn: Dr. James S. Murday (Code 6170)
Washington, DC 20375

DTNSRDC
Attn: Mr. A. B. Neild, Jr. (Code 2723)
Annapolis, MD 21402

NASA-Lewis Research Center
Attn: Mr. Jim Kiraly (MS 23-2)
21000 Brookpark Road
Cleveland, OH 44135

NASA-Lewis Research Center
Attn: Mr. L. Wedeven (MS 23-2)
21000 Brookpark Road
Cleveland, OH 44135

NASA-Lewis Research Center
Attn: Dr. D. Buckley (MS 23-2)
21000 Brookpark Road
Cleveland, OH 44135

DTNSRDC
Attn: Dr. Earl Quandt, Jr.
Annapolis, MD 21402

Naval Research Laboratory
Attn: B. Rath (Code 6490)
Materials Science Division
Washington, D.C. 20390

Naval Air Systems Command
Attn: R. Schmidt, AIR-311A
Washington, DC 20361

Naval Air Systems Command
Attn: Dr. R. Shumaker, AIR-340
Washington, DC 20361

Office of Naval Research
Attn: David S. Siegel (Code 260)
800 N. Quincy Street
Arlington, VA 22217

Naval Air Development Center
Attn: L. Stallings (Code 6061)
Warminster, PA 16974

Defense Advanced Research Project Agency
Attn: CAPT. S. Wax
1400 Wilson Blvd.
Arlington, VA 22209

Naval Sea Systems Command
Attn: Dr. Frank Ventriglio (Code 05R)
Washington, DC 20362

Naval Air Systems Command
Attn: P. Weinberg, AIR-5304C1
Washington, DC 20361

Marine Corps Development Center
Mobility and Logistics Division
Head, Motor Transportation Branch
Quantico, VA 22134

Commanding General (Code D 074)
Marine Corps Development and Education Command
Quantico, VA 22135

Naval Research Laboratory
Attn: Dr. Irwin L. Singer (Code 6176)
Washington, DC 20375

Air Force Wright Aeronautical Laboratories
Wright Patterson Air Force Base
Attn: C. E. Snyder - MLBT
WPAFB, OH 45433

Naval Air Engineering Center
Attn: P. Ciekurs, PE (Code 92A3)
Lakehurst, NJ 08733

NASA-Lewis Research Center
Attn: H. Sliney (MS 23-2)
21000 Brookpark Road
Cleveland, OH 44135

National Science Foundation
Attn: B. Wilcox; Materials
1800 G. Street N.W.
Washington, DC 20550

National Science Foundation
Attn: E. Marsh; Mechanics
1800 G. Street N.W.
Washington, DC 20550

DOE Energy Conversion/Utilization
Oak Ridge National Laboratory
Attn: J.A. Carpenter, Jr.
P.O. Box X
Oak Ridge, TN 37830

::
RE/431/83/20

431:AWR:fmm
13 Apr 1983

Distribution List - Tribology

University/Others

M. J. Devine
General Technology
2560 Prescott Road
Havertown, PA 19083

E. L. Courtright
Battelle Memorial Institute
Pacific Northwest Laboratories
Richland, WA 99352

Dr. A. W. Ruff
Metallurgy Division
National Bureau of Standards
Washington, DC 20234

Dr. P. Nannelli
Pennwalt Corp.
900 First Ave.
P.O. Box C
King of Prussia, PA 19406

Dr. N. P. Suh
Massachusetts Institute of Technology
Department of Mechanical Engineering
Cambridge, MA 02139

Dr. Fred J. Tribe
Admiralty Marine Technology Establishment
Holten Heath, Poole, Dorset
U. K. BH166JU

Dr. R. D. Arnell
Department of Aeronautical &
Mechanical Engineering
University of Salford
Salford, U.K. M54WT

Professor K. Ludema
Department of Mechanical Engineering
University of Michigan
Ann Arbor, MI 48105

Professor W. Kenneth Stair
Associate Dean for Research
University of Tennessee
Knoxville, TN 37996

Prof. Heinz G. F. Wilsdorf
Department of Materials Science
Thorntorn Hall B-234
University of Virginia
Charlottesville, VA 22901

Richard Jentgen
Battelle Columbus Laboratories
505 King Avenue
Columbus, OH 43201

Mr. William Glaeser
Battelle Columbus Laboratories
505 King Avenue
Columbus, OH 43201

BHRA Fluid Engineering
Attn: Dr. Bernard S. Nau
Cranfield, Bedford
England MK430AJ

Franklin Research Center
Attn: Mr. Stuart Gassel
20th and Race Street
Philadelphia, PA 19103

Wear Sciences
Attn: Mr. Marshall Peterson
925 Mallard Circle
Arnold, MD 21012

Westinghouse R&D Center
Attn: Dr. Ian McNab
1310 Beulah Road
Pittsburgh, PA 15235

Mr. Edward L. Wiehe
TRW, Inc.
1 Space Park
Redondo Beach, CA 90278

Professor Ralph A. Burton
Chairman, Mechanical and Aerospace
Engineering Department
North Carolina State University
3211 Broughton Hall
Raleigh, NC 27650

Professor N. S. Eiss, Jr.
Department of Mechanical Engineering
Virginia Polytechnic Institute
and State University
Blacksburg, VA 24061

Professor I. Etsion
Department of Mechanical Engineering
Technion, Haifa 32000
Israel

Professor Hasselman
Virginia Polytechnic Institute
Department of Materials Engineering
Blacksburg, VA 24061

Professor William F. Hughes
Mechanical Engineering Dept.
Carnegie Mellon University
Pittsburgh, PA 15213

Professor Frederick D. Ju
Bureau of Engineering Research
University of New Mexico
Albuquerque, NM 87131

Professor T. Keith
Department of Mechanical Engineering
University of Toledo
Toledo, OH 43606

Professor Francis E. Kennedy, Jr.
Thayer School of Engineering
Dartmouth College
Hanover, NH 03755

Professor Alan O. Lebeck
Mechanical Engineering Dept.
University of New Mexico
Albuquerque, NM 87131

Professor Frederick F. Ling
Department of Mechanical Engineering
Rensselaer Polytechnic Institute
Troy, NY 12181

Dr. Thomas Dow
North Carolina State University
Mechanical and Aerospace Engineering Dept.
Raleigh, NC 27650

Dr. Doris Kuhlmann-Wilsdorf
University of Virginia
Department of Physics
Charlottesville, VA 22901

Dr. David A. Rigney
Ohio State University
116 W. 19th Avenue
Department of Metallurgical Engineering
Columbus, OH 43210

Dr. D. L. Taylor
Cornell University
Mechanical and Aerospace Engineering
Ithaca, NY 14853

Dr. P. W. Whaley
University of Nebraska
223 Bancroft Bld.
Lincoln, NB 68588

Dr. C. Cusano
University of Illinois
Mechanical Engineering Dept.
1206 W. Green Street
Urbana, IL 61801

Mr. Robert Maurer
SKF Technology Services
P.O. Box 515
1100 First Ave.
King of Prussia, PA 19406

Dr. Charles F. Fisher, Jr.
Engr. Experimental Station
University of Tennessee
Knoxville, TN 37996

Westinghouse R&D Center
Attn: Mr. O. S. Taylor
1310 Beulah Road
Pittsburgh, PA 15235

Westinghouse R&D Center
Attn: Dr. P. Reichner
1310 Beulah Road
Pittsburgh, PA 15235

Dr. W. Winer
Georgia Institute of Technology
Mechanical Engineering Dept.
Atlanta, GA 30332

Dr. F. Lockwood
Martin-Marietta Labs
1450 S. Rolling Rd.
Baltimore, MD 21227

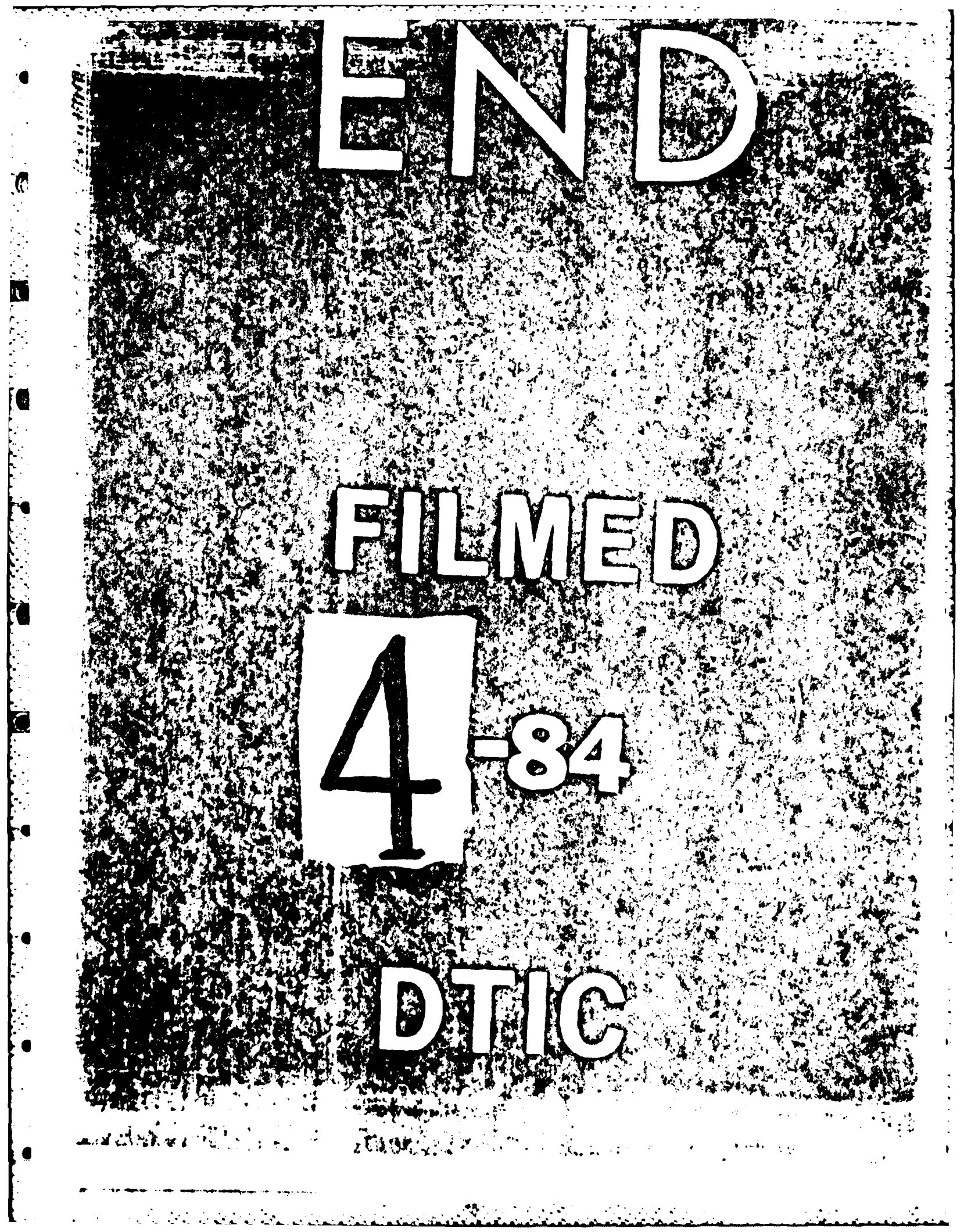
END
FILMED
4-84
DTIC